The International Journal of Cardiovascular Imaging (2006) 22: 457–475
DOI 10.1007/s10554-005-9037-8

Coarctation of the aorta: pre and postoperative evaluation with MRI and MR angiography; correlation with echocardiography and surgery

D. Didier[1], C. Saint-Martin[1], C. Lapierre[1], P. T. Trindade[2], N. Lahlaidi[3], J. P. Vallee[1], A. Kalangos[3], B. Friedli[4], M. Beghetti[4]
[1]*Department of Radiology, University Hospital of Geneva, Geneva, Switzerland;* [2]*Division of Cardiology, University Hospital of Geneva, Geneva, Switzerland;* [3]*Division of Cardiac Surgery, University Hospital of Geneva, Geneva, Switzerland;* [4]*Department of Pediatrics, Pediatric Cardiology Unit, Geneva, Switzerland*

Received 4 May 2005; accepted in revised form 8 September 2005

Key words: aortic coarctation, contrast enhanced MR angiography, Doppler Echocardiography, MR imaging, surgery

Abstract

Aims: To compare MRI and MRA with Doppler-echocardiography (DE) in native and postoperative aortic coarctation, define the best MR protocol for its evaluation, compare MR with surgical findings in native coarctation.*Materials and methods*: 136 MR studies were performed in 121 patients divided in two groups: Group I, 55 preoperative; group II, 81 postoperative. In group I, all had DE and surgery was performed in 35 cases. In group II, DE was available for comparison in 71 cases. MR study comprised: spin-echo, cine, velocity-encoded cine (VEC) sequences and 3D contrast-enhanced MRA.*Results*: In group I, diagnosis of coarctation was made by DE in 33 cases and suspicion of coarctation and/or aortic arch hypoplasia in 18 cases. Aortic arch was not well demonstrated in 3 cases and DE missed one case. There was a close correlation between VEC MRI and Doppler gradient estimates across the coarctation, between MRI aortic arch diameters and surgery but a poor correlation in isthmic measurements. In group II, DE detected a normal isthmic region in 31 out of 35 cases. Postoperative anomalies (recoarctation, aortic arch hypoplasia, kinking, pseudoaneurysm) were not demonstrated with DE in 50% of cases.*Conclusions*: MRI is superior to DE for pre and post-treatment evaluation of aortic coarctation. An optimal MR protocol is proposed. Internal measurement of the narrowing does not correspond to the external aspect of the surgical narrowing.

Abbreviations and acronyms: 3D CE MRA – three-dimensional contrast-enhanced Magnetic Resonance Angiography; BFFE – balanced fast field-echo sequence; Cine MIP – cine maximum intensity projection; CT – Computed Tomography; DE – Doppler Echocardiography; GE – gradient-echo sequence; MIP – maximum intensity projection; MPR – multiplanar reformatting; MR – Magnetic Resonance; MRI – Magnetic Resonance Imaging; SR – surface rendering; VEC MRI – velocity-encoded cine Magnetic Resonance Imaging; VR – volume rendering

Introduction

Coarctation of the aorta is the most frequent congenital anomaly of the thoracic aorta, consisting of a narrowing usually located in the juxtaductal aorta, just distal to the left subclavian artery.

Doppler echocardiography (DE) is currently the first imaging modality used, demonstrating the location and the severity of the constriction and has the advantage of estimating noninvasively the pressure gradient across the narrowing [1]. However, a limited acoustic window encountered with DE may lead to non consistent results, while an exact assessment of aortic anatomy and associated malformations is required before surgical or interventional repair [2]. Magnetic resonance imaging (MRI) has been recognized as the noninvasive imaging modality of choice for the evaluation of aortic coarctation before repair, frequently superior to DE [3–5]. In addition to obtaining morphologic results similar to angiography (site, degree and extent of the narrowing, associated aortic arch tubular hypoplasia and collateral pathways), MRI, with the help of velocity-encoded cine (VEC) technique, can provide quantitative assessment of flow velocities in all segments of the thoracic aorta [6–8]. Additionally, with the use of contrast-enhanced 3D MR angiography (CE MRA), almost all the questions before planning the treatment may be answered [9, 10], making conventional catheter angiography unnecessary or limited to specific indications such as percutaneous interventions.

After repair, close follow-up is mandatory in order to discover postoperative complications, well known for their poor clinical expression [11]. In late childhood and adults, DE, limited by the narrowed acoustic window due to scars, sternal wires, lung interposition and thoracic deformation, remain difficult as well [12], and MRI appeared to be the most effective technique to diagnose postoperative complications in patients following coarctation repair [13].

The purpose of this retrospective study was to compare MRI and MRA findings with DE in a large series of patients with native and postoperative aortic coarctation and, based on our experience, to try to define what is the best MR protocol for its evaluation. The second aim of this study was to compare MR results with surgical findings in native coarctation. To our knowledge, comparison between MR and surgical findings has not been reported.

Material and methods

Patient population

Between 1995 and 2004, a total of 136 MR studies were performed in 121 patients (76 males and 45 females). They were divided in two groups: Group I included 55 preoperative MR studies in 55 patients and group II, 81 postoperative MR studies in 66 patients (10 patients had more than one study in this group II).

In group I ($n = 55$), the mean age at the first MR study was 10.6 years (4 days-30 years) with 20 patients under 2 years. Among these 55 patients who underwent an MR study, all had preoperative DE, 14 had preoperative cardiac catheterization and angiography and surgery was performed in 35 cases, allowing anatomic comparison between surgical and MR findings. 20 patients were not operated because the degree of coarctation was deemed insignificant ($n = 9$), because of operative contraindications ($n = 3$) and moderate hypoplasia of the aortic arch without hypertension and significant stenosis ($n = 6$). Percutaneous angioplasty was performed in one case and one patient was lost for follow-up.

In group II ($n = 81$ in 66 patients), the mean age at the first follow-up study was 15.3 years (2 months-50 years) and the MR study was performed from one week to 32 years after surgery (mean time: 9 years). Primary repair of the coarctation consisted in resection and end-to-end anastomosis in 39 cases, resection with a subclavian flap aortoplasty (Waldhausen procedure) in 15 cases, Dacron patch aortoplasty in 8 cases and balloon angioplasty in 4 cases. 9 patients had two MR studies to follow-up a postoperative residual arch hypoplasia or an asymptomatic recoarctation. In 3 patients, MR study was repeated three times because of the presence of a false aneurysm that recurred in a

young adult and because of the presence of a recoarctation treated by angioplasty and stent in two patients.

In both groups, transthoracic DE was performed without sedation or anesthesia, using VingMed system 5; ultrasound system mainly with 2.5, 5 and 7 MHz transducers for pediatric patients and Sonos 5500; Philips; Andoven MA with an S3 probe for adults.

MR imaging techniques

All MR studies were performed on a 1.5 Tesla magnet (Marconi Eclipse, Cleveland, USA and Philips Intera, Best, Netherlands) using a cardiac coil or the head coil for the younger patients. 2/3 of the 136 MR studies were performed after 2001. Children under 6 years of age were sedated, using Propofol (Diprivan) in continuous perfusion with the help of an anaesthesiologist, allowing rapid and deep sedation with rapid recovery. ECG signal, respiratory curve and oxygen saturation were monitored with the help of a MR compatible system. The different imaging techniques used for the study included: spin-echo and/or fast spin-echo, cine, velocity-encoded sequences and 3D CE MRA.

ECG-gated multislice spin-echo or fast spin-echo black blood images were initially acquired in the axial plane. Then, two additional planes were acquired: coronal and oblique sagittal encompassing the aortic arch. In adults and older children, this sequence was replaced by breath-hold turbo spin-echo black blood sequence with parallel acquisition technique allowing decreasing the scan time with the same spatial resolution. Slice thickness was varying from 3 to 10 mm according to the patient's heart size. In younger patients, large matrix such as 256×512 in the read direction was used, allowing improving spatial resolution without prolongation of acquisition time.

Then, cine-MR imaging was done using segmented gradient-echo (GE) pulse sequences described earlier [14], replaced after 2001 by balanced Fast field echo sequences (bFFE). 16–25 frames covering the cardiac cycle were displayed in a cine loop allowing a dynamic approach. In all cases, oblique sagittal plane encompassing the aortic arch was performed, completed in some cases by an oblique coronal plane centered on the aortic isthmus. The narrowing corresponding to the coarctation was evaluated on diastolic images. Attention was paid on systolic images to show the flow void due to turbulence and acceleration of flow within normally high signal intensity of the blood pool at the level and below the coarctation. At the beginning of the study, from 1995 to 2001, when using GE sequences with a TE = 12 ms, the severity of the narrowing was qualitatively assessed by showing the size and length of this signal void immediately distal to the coarctation [14]. At this time, whereas 3D CE MRA was not yet available, several adjacent oblique sagittal planes with partial overlap were acquired, subsequently reconstructed with the Maximum Intensity Projection algorithm (cine-MIP). This technique described earlier [15], permitted to obtain a resulting image corresponding to the sum of the adjacent planes shown in a cine loop as a standard cine. It allowed the display of the entire thickness of the vessel and added a volume effect whereas the flow information provided by the cine sequence was maintained and was particularly interesting in case of tortuous course of the aorta, very often associated with coarctation. After 2001, GE sequence was replaced by bFFE sequence. The short TE employed in this sequence (TE = 1–2 ms) decreased dramatically the visibility of the signal void. Consequently, the assessment of its length and size was abandoned.

Next, velocity-encoded cine MR (VEC-MR) images were acquired for quantification of the pressure gradient across the coarctation. The calculation of the peak velocity or maximum velocity (V_{max}) within the stenotic jet was performed on planes parallel to the direction of the flow void (in-plane velocity measurement) on oblique sagittal and coronal planes encompassing the length of the jet, with velocity encoded vertically and planes perpendicular to the direction of the flow void (through-plane velocity measurement) on axial transverse images distal to the coarctation in cases where the measurement on the two previous planes was insufficient. The pressure gradient (ΔP) across the narrowing was derived using the modified Bernoulli equation: $\Delta P = 4.\ (V_{max})^2$ where ΔP is the pressure drop across the stenosis and V_{max} the

peak velocity in m/s measured within the stenotic jet.

At the end of the examination, 3D CE MRA was performed after a small test bolus injection (2 ml) of Gadolinium to determine the arrival time of the contrast in the thoracic aorta. Acquisition was realized two times in two breath-hold periods and was oriented in the oblique sagittal plane encompassing the entire thoracic aorta. Each acquisition time was 16 s. The contrast material was Gadolinium DTPA (Schering, Berlin, Germany) or DOTA (Guerbet, Paris, France) at a dose of 0.2 mmol/kg body weight and a contrast injection rate of 3 ml/s. Contrast medium was injected with an MR compatible infusion pump (Medrad Spectris, Pittsburg Pa.) in an antecubital vein, flushed by 20 ml of saline. For patients under 3 years of age, the contrast medium was injected manually just after a bolus of Propofol (Diprivan) to obtain an apnea during the 32 s of acquisition. At the end of the MRA study, the patient was immediately taken out of the magnet and manually ventilated by the anesthesiologist and recovery of spontaneous ventilation took about 5 min. The source images of CE MRA were analyzed on a computer workstation (Twinstar, Marconi, Cleveland, USA or Vitrea 2, Vital Images, Plymouth, MN) and immediately reconstructed, using maximum intensity projection (MIP), multiplanar reformatting (MPR) and 3D surface (SR) or volume rendering (VR) algorithms. The total MR study was 30–45 min.

Image analysis and comparison with other techniques and surgical findings

In the group I, image analysis consisted in demonstrating the site, the length and the degree of the coarctation, the distance to the subclavian artery, the association with tubular hypoplasia of the aortic arch and the presence of collaterals as well as associated malformations. The degree of the stenosis was considered as severe if the ratio of the coarctation diameter to the distal descending aortic diameter was <0.5 [16] and/or peak systolic gradient greater than 40 mm Hg [17]. The length of the coarctation was considered as short if the length of the narrowed aortic segment was <0.5 cm and long if the length of the narrowed aortic segment was >0.5 cm [18]. The aortic arch was considered as hypoplastic when the ratio of transverse aortic arch diameter to distal descending aorta diameter was <0.9 [13].

Measurements of the internal vessel diameters were carried out by two experienced radiologists (DD and CSM), either on spin-echo, cine or CE MRA source and/or reconstruction images, where the best view of the entire lumen of the considered segment was demonstrated. The aortic arch diameter was measured between the left common carotid and the subclavian arteries. The subclavian diameter was measured at the origin of the vessel. The measurement of the isthmic coarctation was performed where the smallest internal diameter of the constricted segment was demonstrated and compared with the distal descending aortic diameter. The post-stenotic aortic diameter was measured on the first centimeters of the thoracic descending aorta. These data were compared with the anatomic description during surgery. The same measurements were performed in the patients who underwent surgical repair. Prior to the cross-clamping of the aorta proximal and distal to the coarctation, external measurements were done using a compass applied around the distal arch, the origin of the left subclavian artery, the isthmus, as well as the first centimeters of the descending aorta and reported to a rule.

Morphologic results of MR findings were compared in all cases of this group with Doppler echocardiography results. Estimate of the pressure gradients across the coarctation with VEC MR sequences was compared with the results of Doppler echocardiography in 28 cases. Catheterization was only performed in 14 cases, but comparison of the results with VEC MR pressure gradients was not done because only 4 patients had both catheterization and MR data available.

Comparison between MR and surgical findings and comparison between pressure gradients estimates in MR and Doppler echocardiography were done using linear regression analysis. Mean differences and limits of agreement were calculated according to the method proposed by Bland and Altman.

In the group II, image analysis consisted in demonstrating residual pathology or complications such as aortic arch configuration and diameter abnormalities, recoarctation, abnormal angulation or course, aortic wall and aortic side branches abnormalities. Aortic pathology was mainly qualitatively assessed, taking into account accepted standards defining thoracic aorta abnormalities [19, 20] and compared with Doppler echocardiographic results.

Results

Group I

MR findings: Transverse axial spin-echo or Fast spin-echo images at the level of the aortic arch and the isthmus identified the narrowing in 1/4 of the cases, particularly in long segment coarctation but it was not demonstrated in 3/4 of the cases on this plane because it was obscured by a partial volume effect, particularly in young children. However, this plane permitted the definition of the oblique sagittal plane of the aorta in the thorax and associated anomalies. The entire thoracic aorta was optimally visualized on this oblique sagittal plane in 2/3 of the cases. The coarctation appeared as a focal shelf-like deformity of the isthmus in cases of short coarctation and a long segment narrowing in cases of long coarctation. The associated tubular hypoplasia of the aortic arch was usually perfectly demonstrated on this plane (Figure 1).

But in 1/3 of the cases, despite a supposedly good alignment with the aortic arch, the narrowing could not be demonstrated on a single oblique sagittal plane because of the displacement of a portion of the thoracic aorta due to the coarctation and very commonly associated tortuous course of the vessel. Only the coronal or oblique coronal plane encompassing the origin of the descending aorta permitted the demonstration of the narrowing (Figure 2).

On oblique sagittal cine images, the narrowing corresponding to the coarctation was better evaluated on diastolic images, whereas on systolic images it was partially obscured by the signal void due to high-velocity turbulent flow across the coarctation, particularly on GE sequences employed at the beginning of the study. In some cases, collaterals could be demonstrated as well (Figure 3).

In 1/3 of the cases, because of the kinking of the aorta, only parts of the aortic arch were visualized

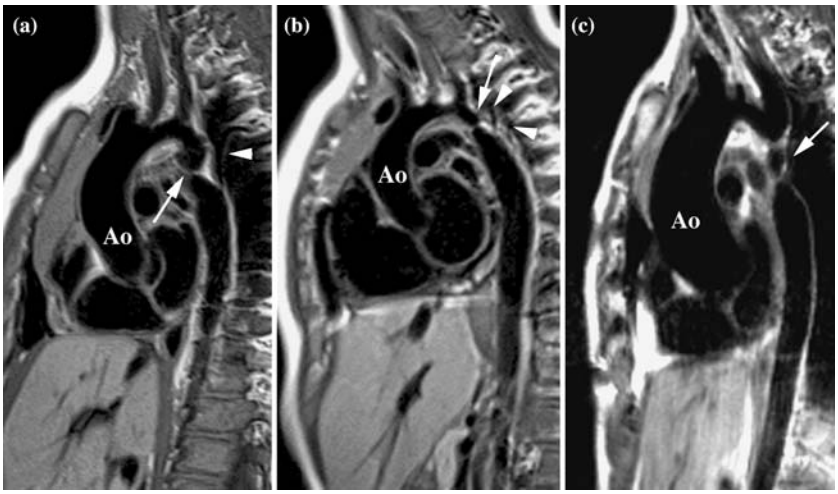

Figure 1. Three examples of tight coarctation (arrows) demonstrated on oblique sagittal plane spin-echo images where the entire thoracic aorta was optimally visualized. The coarctation appeared as a focal shelf-like deformity of the isthmus in cases of short coarctation (a, b) and a long segment narrowing in cases of long coarctation (c). The associated tubular hypoplasia of the aortic arch is perfectly demonstrated on this plane as well as collaterals (arrowheads). A_o = ascending aorta.

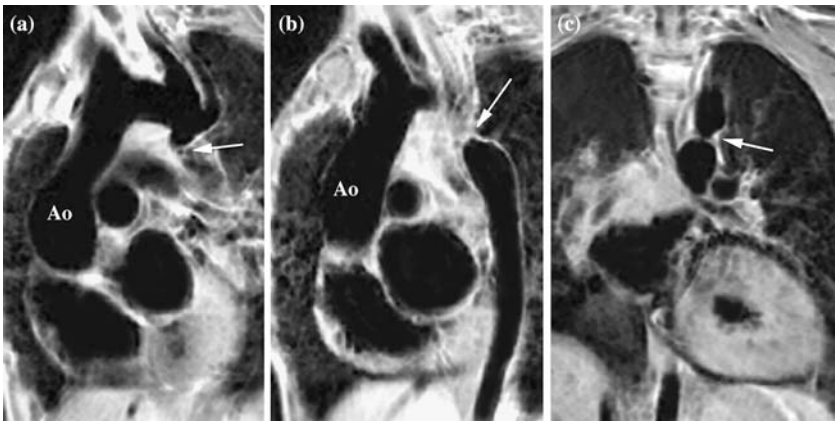

Figure 2. Example of a tortuous course of the aortic arch. Despite a supposed good alignment with the aortic arch, the narrowing cannot be demonstrated on a single oblique sagittal plane (a, b) and only the coronal plane encompassing the origin of the descending aorta permits the demonstration of the narrowing (c) (arrows). A_o = ascending aorta.

on a single plane, requiring using the cine-MIP algorithm reconstruction of several adjacent oblique sagittal planes, described above, to image the entire aortic arch (Figure 4).

The oblique sagittal and the coronal planes were usually optimal for the direct measurement of increased flow velocity within the stenotic jet demonstrated on cine images by VEC sequences (Figure 5).

In cases where the jet was very narrowed, the measurement of maximum velocity was not possible on oblique sagittal plane because of partial

Figure 3. Oblique sagittal systolic cine images of a short (a) and a long (b) coarctations. The signal void due to high-velocity turbulent flow across the coarctation is well demonstrated (arrow). The severity of the narrowing can be qualitatively assessed by the length and the size of the signal void immediately distal to the coarctation. Collaterals are well visualized as well (arrowheads).

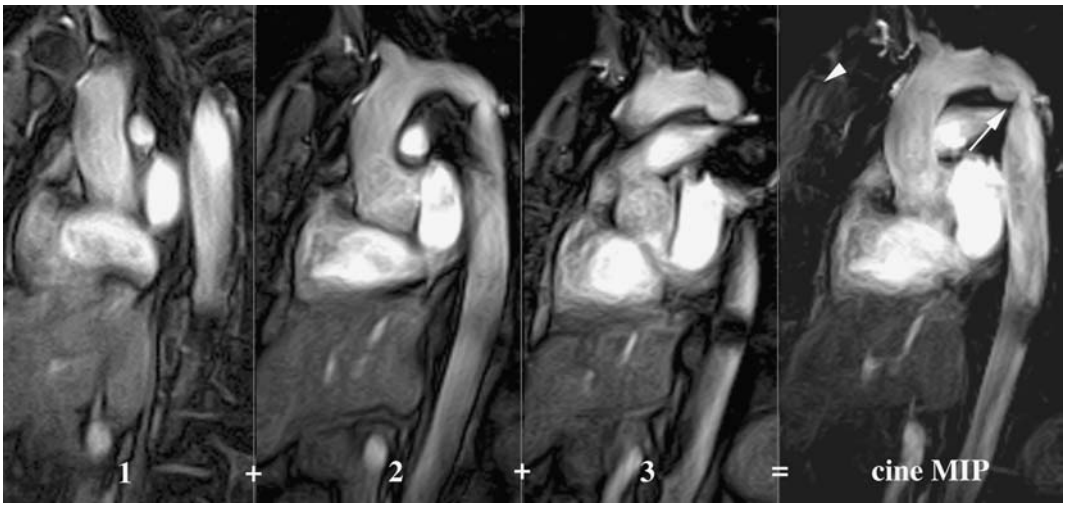

Figure 4. Oblique sagittal diastolic cine images of a moderate coarctation. In this case, because of the kinking of the aorta, only parts of the aortic arch are visualized on a single plane (1, 2, 3), requiring using subsequent reconstruction of these three planes with the cine-MIP algorithm to image the entire aortic arch and to display the narrowing (arrow). Superimposition of the three planes is shown on anterior thoracic wall (arrowhead).

volume averaging and motion of the jet out of the imaging plane but this measurement was usually possible on the additional coronal plane. In these difficult cases, additional through-plane measurement on transverse images distal to the coarctation was carried out. In two cases of very tight stenosis, calculation of maximum velocity remained impossible because the flow was insufficient distal to the

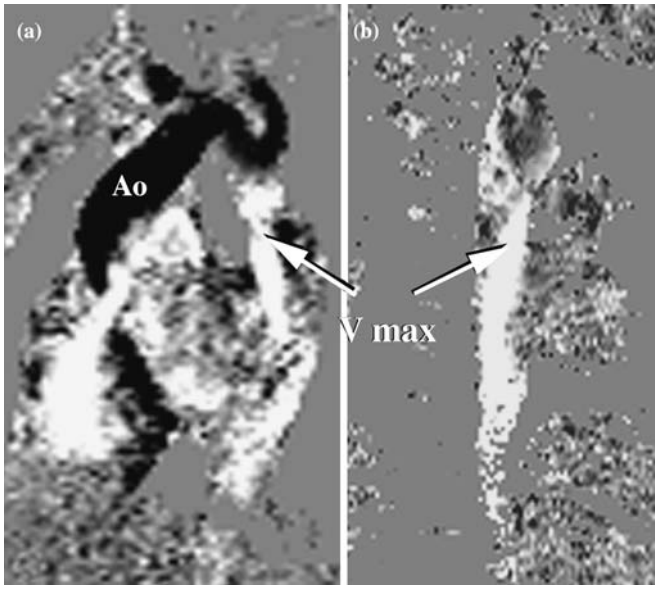

Figure 5. VEC images in oblique sagittal (a) and coronal (b) planes in a patient with severe coarctation. These two planes are usually optimal for direct measurement of increased flow velocity (V_{max}) within the stenotic jet (arrow) demonstrated on cine sequences. A_o = ascending aorta.

coarctation and preferentially directed to the collateral circulation.

Gadolinium-enhanced MR angiography was the best technique to image the entire thoracic aorta and to display the aortic malformation. Oblique MPR and volume rendering reconstructions were optimal to display the collateral circulation (Figure 6).

Based on these imaging techniques, results of MRI evaluation in the 55 patients of group I were the following:

- The degree of the stenosis was considered as severe in 39 cases and moderate in 16 cases,
- The length of the coarctation was short in 46 cases and long in 9 cases,
- Associated tubular hypoplasia of the aortic arch was present in 26 cases,
- Collateral circulation was found in 35 out of the 39 cases (89%) with severe stenosis. It was always absent in moderate stenoses,
- Associated anomalies comprised: complex anomalies and cono-truncal malformations ($n=11$), left-to-right shunts ($n=10$), right aortic arch ($n=1$), aberrant right subclavian artery ($n=2$), bicuspid aortic valve ($n=7$), left superior vena cava ($n=3$), ductus arteriosus ($n=7$), pulmonary stenosis ($n=2$).

Comparison of MRI and Doppler echocardiography results

Among the 55 preoperative patients, the definitive diagnosis of coarctation was made by Doppler echocardiography in 33 cases and suspicion of coarctation and/or aortic arch hypoplasia in 18 cases. The aortic arch was not well demonstrated in 3 cases and one case was missed by Doppler echocardiography.

VEC MRI and Doppler estimates of pressure gradients across the coarctation were available for comparison in 28 cases. The VEC MRI estimates of pressure gradient are plotted against the Doppler estimates in Figure 7. The graph indicates a good correlation between the two methods ($r=0.71$). Doppler measurement was impossible in 3 cases and MRI measurement was impossible

Figure 6. Oblique thick-slab MPR (a) and volume rendering (b) reconstructions of a Gadolinium-enhanced MR angiography are the best techniques to image the entire thoracic aorta and to display the aortic coarctation (arrow). They are optimal to display the collateral circulation as well (arrowheads).

in 2 cases as mentioned above. It was mainly due to the presence of a tight stenosis and the flow below the coarctation was not detectable because it was preferentially directed to the collateral circulation.

Comparison of MR and surgical results

Comparison of MR and surgical results are summarized on Table 1. Among the 35 patients out of the 55 patients of the group I who underwent surgical repair, the comparison between morphologic appearance of the malformation during surgery with preoperative MRI results was excellent.

Surgical measurements of all parts of the aortic arch and isthmic region were not available in all 35 operated cases. Comparison with MRI measurements was done only in 20 cases at the level of aortic arch, in 15 cases at the level of isthmic region and in 19 cases at the level of descending aorta. The MRI measurements of aortic arch and isthmic aortic diameters are plotted against the same measurements carried out during surgical repair on Figures 8 to 9. The graphs indicate a close correlation between MRI and surgery in the measurements of aortic arch diameters ($r = 0.93$) but a very poor correlation in measurements of isthmic coarctation ($r = 0.24$). A close correlation was found as well in the measurements of subclavian artery ($r = 0.84$) and post-stenotic aortic diameter ($r = 0.82$) (not shown).

Group II

Among the 81 postoperative MR studies done in the 66 patients of the group II, only one was rejected because of poor image quality due to patient motion during the examination. Doppler echocardiography was not done in 9 cases and available for comparison in only 71 cases but was limited by a poor acoustic window in 3 of these cases. MR study demonstrated a good surgical result with a normal diameter in the coarctation region in 39 studies (ratio of the diameter of the isthmic region to distal descending aortic diameter between 0.9 and 1.5) [13]. Persistence or recurrence of a narrowing in the coarctation region (ratio of the diameter of the isthmic region to distal descending aortic diameter < 0.9) was found in 20 studies (Figure 10).

In 10 of them, the narrowing was mild (ratio of the diameter of the isthmic region to distal descending aortic diameter between 0.9 and 0.6). In all of these cases, the narrowing had little influence on blood flow (Pressure gradient

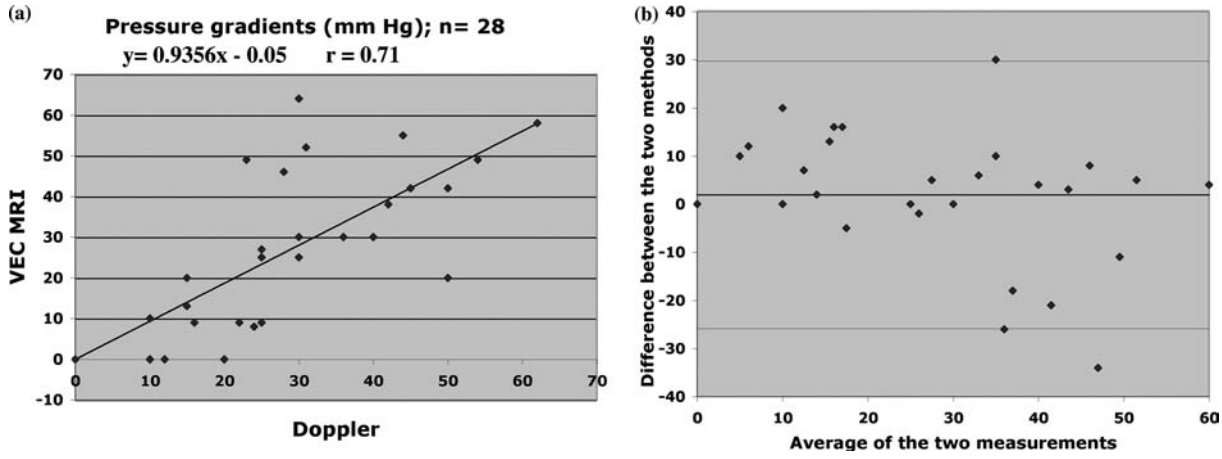

Figure 7. (a) Comparison by linear regression of pressure gradients estimates obtained by VEC MRI and Doppler Echocardiography. MR measurements are plotted against the Doppler measurements. The graph indicates a good correlation between the two methods ($r = 0.71$). (b) Difference between MRI and Doppler measurements is plotted against the mean value of each pair according to the Bland and Altman method. Thick line represents mean difference; thin lines show the limits of agreement (± 2 SD).

Table 1. MRI and Surgical morphologic analysis of the coarctation; ($n = 35$).

	Length of stenosis			Degree of stenosis			Hypoplasia of aortic arch	
	Short	Long	Unknown	Moderate	Severe	Unknown	Presence	Absence
MRI	26	9	–	5	30	–	18	17
Surgery	24	10	1	6	26	3	17	18

≤30 mm Hg on VEC cine MRI and Doppler measurements). In 5 of them, the narrowing was moderate (ratio of the diameter of the isthmic region to distal descending aortic diameter between 0.6 and 0.4). In two of these cases, the pressure gradient was >30 mm Hg on VEC cine MRI and Doppler measurements (33 and 36 respectively). In the 5 remaining studies the stenosis was considered as tight (ratio of the diameter of the isthmic region to distal descending aortic diameter <0.4). The pressure gradient was >40 mm Hg on VEC cine MRI and Doppler measurements and collateral circulation was present in 3 of these cases. Persistence of tubular hypoplasia of the aortic arch was found in 18 cases. It was always mild to moderate (ratio of the transverse aortic arch diameter to distal descending aortic diameter between 0.9 and 0.5) (Figure 11).

Flow disturbance was always encountered as a discrete to moderate flow void on oblique sagittal cine images, and pressure gradient >30 mm Hg on VEC cine MRI was seen in 4 cases. Concomitant abnormal angulation of the aortic arch was found in 10 cases with extreme kinking in 6 cases.

Abnormal flow was encountered as well in these cases with flow void on oblique sagittal cine images and pressure gradients >30 mm Hg on VEC cine MRI in 4 studies (Figure 10, 11).

In two studies, a pseudoaneurysm was discovered at the level of isthmic region (Figure 12).

All these anomalies were better demonstrated on CE MRA. Thick-slab MPR and volume rendering reconstructions were optimal to display these postoperative complications (Figures 11, 12). In the two patients treated by stent implantation, because of the artifacts generated by the stent, it was

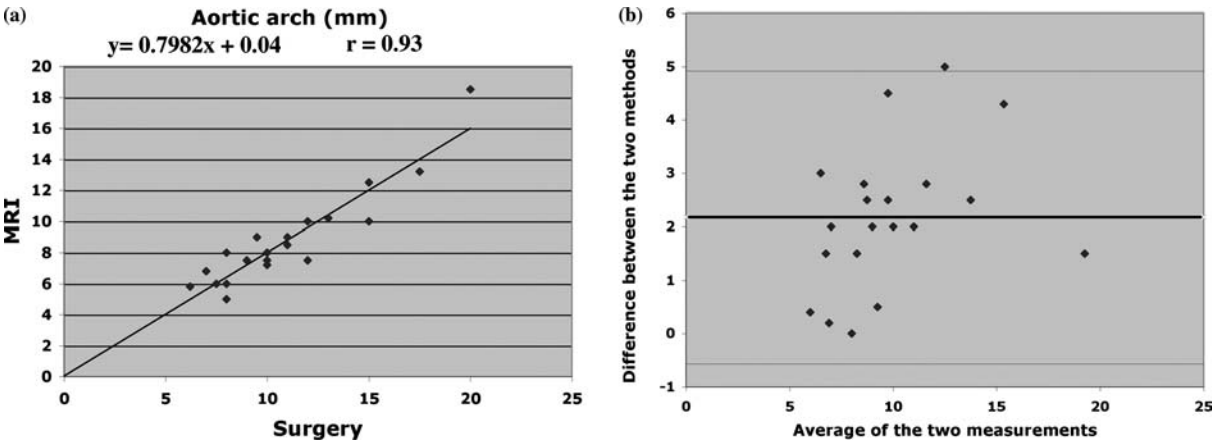

Figure 8. (a) Comparison by linear regression of aortic arch diameter measured by MRI and surgery ($n = 20$). MRI measurements are plotted against the same measurements performed during surgical repair. The graph indicates a close correlation between MRI and surgery in the measurements of aortic arch ($r = 0.93$). (b) Difference between MRI and surgical measurements is plotted against the mean value of each pair according to the Bland and Altman method. Thick line represents mean difference; thin lines show the limits of agreement (±2 SD).

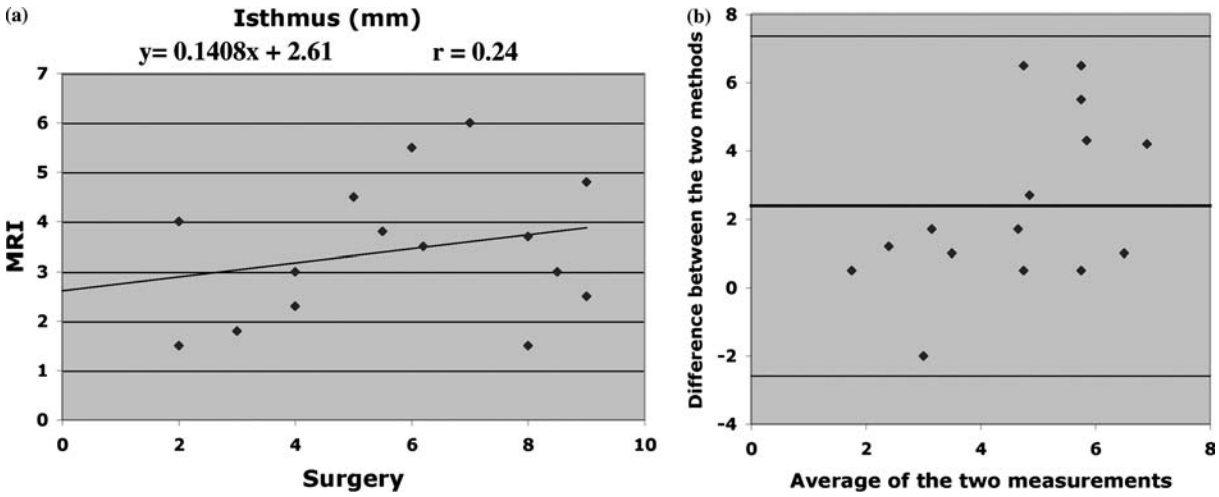

Figure 9. (a) Comparison by linear regression of isthmic diameter measured by MRI and surgery ($n = 15$). MRI measurements are plotted against the same measurements performed during surgical repair. The graph indicates a poor correlation between MRI and surgery in the measurements of isthmic region ($r = 0.24$). (b) Difference between MRI and surgical measurements is plotted against the mean value of each pair according to the Bland and Altman method. Thick line represents mean difference; thin lines show the limits of agreement (± 2 SD).

difficult to evaluate the result after treatment either with spin-echo or MR angiographic images. In these cases, a multislice gated CT was performed.

Comparison of MRI results of the group II with Doppler echocardiography is summarized on Table 2.

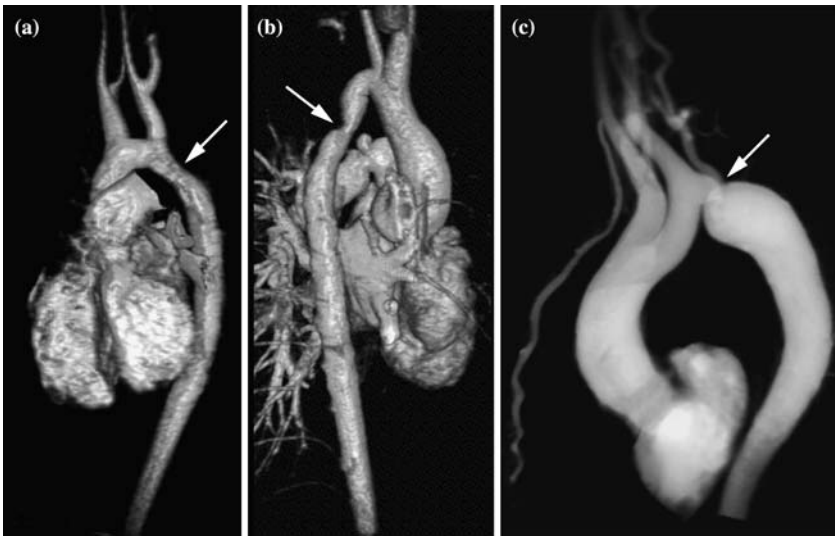

Figure 10. Surface rendering (a, b) and volume rendering (c) reconstructions of a Gadolinium-enhanced MR angiography in post-operative patients. On (a), there is a slight non significant residual stenosis. Subclavian artery has been anatomosed to the left carotid artery. On (b), a 50% narrowing is demonstrated associated to a kinking of the aortic arch. On (c), a tight recoarctation is shown with severe hypoplasia of the aortic arch and the subclavian artery (arrows) and kinking. Note dilated internal mammarian artery.

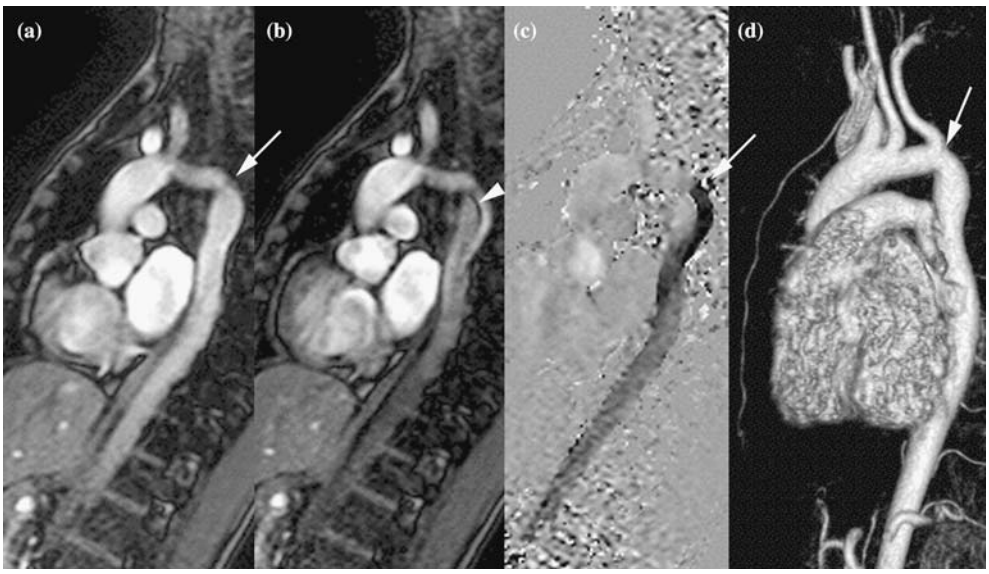

Figure 11. Oblique sagittal diastolic (a) and systolic (b) cine images, corresponding VEC image (c) in the same plane and surface rendering reconstruction of a Gadolinium-enhanced MR angiography (d) after coarctation repair. Despite the good result at the level of the isthmus (arrows) demonstrated by MRA, persistence of aortic arch hypoplasia and kinking are responsible for presence of a flow void on systolic image (arrowhead) and acceleration of flow on VEC image (3 m/s).

Among the 71 studies available for comparison between the two techniques, a normal appearance of the coarctation region was detected by DE in 31 out of 35 cases. Among the 17 cases where MRI found a narrowing or a recoarctation, 8 cases were detected by DE, only an abnormal flow was

Figure 12. Oblique sagittal spin-echo (a) and cine-MIP image (b) after coarctation repair demonstrate a huge pseudoaneurysm (arrows) at the level of the previous isthmic coarctation.

detected by DE in 4 cases and DE was considered as normal in 5 cases. Aortic arch tubular hypoplasia was demonstrated by DE in only 9 out of 16 cases (tubular hypoplasia was associated or not associated with narrowing or recoarctation). Kinking of the aortic arch was shown by DE in only 4 out of 10 cases. One of the two pseudoaneurysms was not detected as well.

Discussion

MRI is the noninvasive method of choice for evaluating the morphology of aortic coarctation and particularly to depict the location, the degree and the length of the narrowing, the degree of associated aortic arch hypoplasia, the presence of collateral circulation, the poststenotic dilatation and the relationship to the left subclavian artery; all these parameters are necessary to plan surgical or interventional repair [21–23]. MRI also appears to be the most effective technique to follow-up patients after coarctation repair and diagnose postoperative complications [13, 15].

Complete MR examination requires numerous sequences to provide evaluation of both anatomic and hemodynamic severity of the coarctation.

Morphologic assessment of the aortic malformation

Gated Fast spin-echo and Turbo spin-echo sequences remain the first step in the depiction of abnormal morphology. Transverse axial plane is not the ideal incidence for identifying the narrowing because it is often obscured by a partial volume effect, particularly in young children. However, this plane is necessary because it permits the definition of the oblique sagittal plane of the aorta in the thorax and is essential to demonstrate associated anomalies. The oblique sagittal plane encompassing the entire thoracic aorta is usually the best to demonstrate the coarctation and the associated tubular hypoplasia of the aortic arch. But in 1/3 of the cases of our series, despite a supposedly good alignment with the aortic arch, the narrowing cannot be demonstrated on a single oblique sagittal plane because of the displacement of a portion of the thoracic vessel, which is due to the coarctation and the very commonly associated tortuous course of the aorta. In theses cases, only the coronal or oblique coronal plane encompassing the origin of the descending aorta permits the demonstration of the narrowing. The importance of multiple imaging planes has been mentioned previously [24], indicating that these two latter planes are complementary and more sensitive for the depiction of the anomaly.

The cine sequence usually follows spin-echo imaging and the optimal plane to depict the coarctation is the oblique sagittal plane identical to the plane described above. The narrowing corresponding to the coarctation is better demonstrated on diastolic images whereas the importance and extension of the flow void immediately distal to the coarctation is appreciated on systolic images. The size and the length of the flow void are good indicators of the severity of the stenosis [25, 15]. However, the cine technique is of importance. The segmented *k*-space gradient echo sequence (GE), only used at the beginning of the study gave the better results on the visualization of the signal

Table 2. Comparison of MRI and Doppler Echocardiography results in the postoperative group II; ($n = 71$).

$n = 71$	Doppler Echocardiography						Poor window
MRI	Normal	Narrowing Recoarctation	Tubular Hypoplasia	Abnormal Flow	Kinking	PSA	3
Normal (35)	31	0	0	2	0	0	2
Narrowing Recoarctation (17)	5	8	0	4	0	0	0
Tubular hypoplasia (16*)	3	0	9	3	0	0	1
Kinking (10)	4	0	0	2	4	0	0
PSA (2)	1	0	0	0	0	1	0

*Tubular hypoplasia was associated or not associated with narrowing or recoarctation.

void. This latter is due to high-velocity turbulent flow across the coarctation resulting in spin dephasing on systolic images because of long echo times used (TE = 9–12 ms) with this technique. At present, these sequences have been replaced by steady-state free precession (SSFP) sequences allowing substantial improvement in the quality of images and reduction of acquisition time by a factor of 2–3 compared to the previous technique [26]. On the balanced fast field echo (bFFE) technique performed in this study after 2001, which uses short repetition times (TR = 3–5 ms) and short echo time (TE = 1–2 ms), the appearance of the signal void is clearly diminished compared to GE sequences. One has to keep in mind these different types of techniques when comparing cine images obtained from different scanners. The tortuous course of the aorta may be a problem as well with this technique as mentioned above for spin-echo imaging. This is the reason why at the beginning of the study we applied the "cine-MIP" technique mentioned above, replaced subsequently by MR angiography.

3D CE MRA is at present the technique of choice to demonstrate the malformation. It has been compared with conventional angiography with excellent anatomic correlation in coarctation and other aortic diseases [27–29]. Demonstration of the site, degree and length of the narrowing as well as associated tubular hypoplasia of the aortic arch and collaterals is usually easy even in small children with the help of a bolus of Propofol (Diprivan) injected immediately before Gadolinium administration in order to obtain a short apnea avoiding motion artifacts. This technique necessitates the presence of an anesthesiologist ready to ventilate the patient at the end of the MRA study. Recovery of spontaneous ventilation took usually about 5 min. This technique was very safe and no complications occurred [15]. Tortuous, angulated or kinked course of the aorta is no longer a problem with MRA. First of all, it remains important to review the source images because subtle details of aortic wall and small collaterals may be missed with reconstruction techniques such as MIP. Measurement of the diameter of the different segments of the aorta is usually easy on the source images. MIP is the most widely used reconstruction technique but, because of overlapping of anatomic structures in the thorax MIP is not sufficient to define accurately the degree of the narrowing. The best technique to measure the lumen diameter of the different segments of the aorta was MPR in oblique sagittal, coronal and curve reconstructions. 3D surface (SR) and volume rendering (VR) techniques are more esthetically pleasing than MIP. VR, relying on sophisticated combination of transparency, opacity and colors of the objects is the most efficient technique to display 3D morphology. However, because these techniques rely on thresholding between the object of interest and surrounding structures, they are less efficient in the measurement of the aortic diameters [30].

Measurements of aortic diameters and comparison of MR and surgical results

MRI measurements of aortic diameters have been compared with conventional angiography and echocardiography with an excellent correlation [2, 12, 29, 31, 32]. Angiographic results were compared as well with anatomic measurements with good correlation between the internal diameters of the coarctations measured angiographically and those measured anatomically [20]. However, this study compared the resected coarctation specimen with angiographic data. The angiographic diameters tended to be larger than the anatomic diameters due to the fact that measurements were made on aortas that were distended by systolic arterial pressure whereas anatomic measurements were made on specimen *ex-vivo*. In our study, MRI measurements of the internal vessel diameter were carried out where the best view of the entire lumen of the considered segment was demonstrated, whereas anatomic measurements were made by operative examination before resection and concerned the external diameter of the vessel, including its wall thickness. To our knowledge such a comparison has not been done previously. Despite this difference in the measurements, a close correlation was found for the diameters of aortic arch, subclavian artery and post-stenotic descending aorta ($0.82 < r < 0.93$), the aortic wall being usually thin, particularly in young children. Conversely, a

poor correlation was found between measurements carried out at the level of the isthmic coarctation segment. There are several explanations to this discrepancy. As demonstrated on resected specimens, the aortic lumen is narrowed by elastic tissue which invaginates from the posterior wall of the aorta toward the aortic attachment of the ligamentum arteriosum or ductus arteriosus and this invaginated elastic media is usually thicker on the first centimeters of aorta distal to the narrowing than on the aorta just proximal to the coarctation. Furthermore, fibrous tissue fills the adventitial side of the invagination and frequently accumulates on the intima distal to the invaginated aortic wall due to turbulent blood flow (intimal jet lesion). As a result, the external aortic narrowing including its abnormal wall thickness measured by the surgeon is usually slight compared with the aortic luminal narrowing measured on MR images.

Other reasons of this discrepancy relate to the MRI technique itself. Despite the use of high-resolution spin-echo images (256 × 512 matrix), multiple planes and thin section images, very thin structures may produce little or no MRI signal [15], particularly when acquiring images during normal respiration. Thus, thin portions of the invaginated tissue may be obscured and the residual narrowed lumen is difficult to see in severe coarctations. This is the reason why the measurements were not obtained on spin-echo images only, but on images coming from other sequences as well (cine and MRA images), where the best view of the lumen of the narrowed segment was demonstrated.

Evaluation of the pressure gradient across the coarctation

Several previous studies have demonstrated the good correlation for pressure gradient measurements across the coarctation obtained from Doppler peak velocity measurement and velocity-encoded cine MR technique (VEC) [33–35]. This present study confirmed this good correlation. Guided by the flow void demonstrated on cine-GE images, when available, oblique sagittal and coronal planes parallel to the direction of flow, encompassing the length of the jet, with velocity encoded vertically (in-plane velocity measurement) are optimal for this measurement [36]. It yields numerous pixels for analysis of velocity because the entire abnormal jet is displayed. But in case of very tight stenosis, where the jet is narrowed, particularly in small aortas, in-plane measurement may be less reliable because of partial volume averaging, motion of the jet out of the imaging plane and improper alignment of the jet. In this case, the use of thinner image section may solve the problem. Conversely, with through-plane imaging, only a slice of the jet is displayed and one can miss the maximum velocity if the plane is positioned too far or too close to the origin of the narrowing. Furthermore, misregistration of flow due to signal loss depending upon turbulence and eddy currents may occur if the plane is too close to the origin of the stenosis. Thus, it is preferable to measure data in both in and through-planes [37–39]. Practically, because of the short acquisition time of these sequences, two in-plane velocity measurements (oblique sagittal and coronal) and one or several through-plane velocity measurements (transverse images below the coarctation) must be performed if the two previous in-plane measurements are not consistent or if there is discrepancy between the two measurements.

As mentioned previously, the Doppler velocity measurements give overestimates up to 30% compared with MRI measurements [2, 40, 41]. This can be explained by partial volume effect and velocity measurements only done perpendicular to the direction of flow (through-plane imaging). The discrepancy between MRI and DE results may be explained as well by the conditions of measurements: with sedation during MR study and without sedation during DE study.

Evaluation of collateral circulation

The amount of collaterals is usually proportional to the severity of the coarctation even if, in exceptional cases scarce collaterals may be found with tight coarctations. Demonstration of collateral circulation is of importance before surgical treatment to avoid ischemic medullary injury. In the rare cases of significant coarctations with poor development of collaterals, the surgeon will use

bypass circulation to prevent medullary ischemia during aortic cross-clamp. At present, the best technique to demonstrate collateral circulation is 3D Gadolinium-enhanced MRA that shows dilatation of the internal mammarian, intercostals, posterior mediastinal and cervical arteries on MIP, MPR or volume rendering images [42]. Estimation of collateral circulation can be carried out as well with VEC-MR by measuring flow in the proximal (10 mm below the stenosis) and distal part (at the diaphragm level) of descending aorta. In hemodynamically significant coarctation, there is an $83 \pm 50\%$ increase in flow in the distal compared with the proximal part of the descending aorta, due to the collateral flow, whereas in normal subjects and mild coarctations there is a decrease in total flow from proximal to distal aorta [43]. Collateral flow will be calculated as flow in the distal descending aorta minus flow in the proximal descending aorta [35]. But large collaterals are often entering at the level or immediately below the narrowing as demonstrated on Figure 6 and this flow may influence such measurements [43]. Aortic flow measurements at the diaphragm level may be influenced as well by blood leaving the aorta through the celiac artery [1]. Thus, MR velocity measurements should not be performed when significant collaterals are detected and kept for cases where there is doubt regarding the severity of the stenosis, and in mild or moderate coarctation when collaterals are not visible [43].

Follow-up of patients after coarctation repair

After coarctation repair, either by surgery or balloon angioplasty, regular follow-up examinations are mandatory because complications may occur, even after a long period after treatment, especially when the intervention was performed in neonates. These complications include persistence of hypertension, recurrence of coarctation and aneurysm formation at the site of previous intervention. Their poor clinical expression and their significant morbidity and mortality are the major reasons for a systematic prolonged follow-up [44]. For this purpose, cardiac catheterization and angiography have been replaced by modern noninvasive imaging techniques in many centers [11]. Transthoracic Doppler echocardiography remains the first follow-up screening test and is usually an accurate method in infants and children. However, visualization of the aortic arch and isthmus is frequently suboptimal in adolescents and adults and transthoracic echocardiography may be limited by a narrowed acoustic window due to postoperative scar, lung interposition and thoracic deformation [45, 12]. These patients may benefit from transesophageal echocardiography but many of them do not accept to repeatedly swallow the probe. Moreover, pressure gradients may remain elevated at the coarctation site, even after a successful repair due to the angulation and kinking of the aortic arch and persistence of aortic arch hypoplasia. This is the reason why MRI is at present done routinely as a follow-up screening test after coarctation repair and has been recognized as the most cost-effective technique [46]. According to other studies and to our results, numerous abnormalities and complications after repair were not detected by echocardiography, particularly in adult patients [13]. In this study, narrowing or recoarctation, tubular hypoplasia of the aortic arch and kinking were not detected by DE in about 50% of the cases. Spin-echo imaging remains essential to detect abnormalities of the aortic wall and associated intracardiac anomalies. But the examination must include haemodynamic evaluation by velocity-encoded cine MR and especially Gadolinium-enhanced 3D MRA, which provides the best view of the entire reconstructed aorta [13]. After reviewing the source images, many reconstructions may be performed. Maximum intensity projection technique (MIP), the most widely used technique for visualization of 3D MRA data, provides a resulting image similar to a standard angiographic image. But, because it does not differentiate front from back, adjacent structures may overlap, and due to selection of the highest intensity voxel in the data set, MIP overestimates the degree of narrowing. Volume rendering technique, which relies on a combination of transparency and opacity, permits visualization of low intensity and smaller structures that have a lower contrast ratio and is therefore more efficient to evaluate residual abnormalities of the entire thoracic aorta. Thick-slab MPR, which allows

interactive positioning of an oblique plane across the entire thoracic aorta, gives a better view of the vessel and its branches, particularly in cases of tortuous, angulated and kinked residual morphology. Evaluation of patients treated by stent implantation remains difficult either with spin-echo or MR angiographic images because of the artifacts generated by the stent. In these cases, a multislice ECG gated CT may be performed.

Study limitations

The limitation of this study is that it is a retrospective study, and not all the data were available for comparison. This is the case for gradients estimates that were not performed in all patients, either in DE or MRI; also, measurements were done in different conditions (with and without sedation). These measurements of pressure gradients were performed as well without taking into account the severity-based loss coefficient (K) in the modified Bernoulli equation as described by Oshinski et al. [47] either with DE or VEC MRI. Evaluation of associated bicuspid aortic valve was not systematically done particularly at the beginning of the study, as this would have necessitated additional sequences, especially a standard cine or magnitude reconstruction of VEC cine in the plane of aortic annulus. It is also the case for surgical and MRI comparison. If comparison of MRI data and surgical anatomical results was obtained in 35 cases, surgical measurements of aortic segments were not available in all these cases and analysis of explanted material was not performed. Another limitation of this study is due to the fact that MRI techniques significantly improved, particularly after the development of SSFP cine sequences and 3D MRA. The image quality may be difficult to compare between images done at the beginning of the study and recent MR examinations.

Conclusions

Magnetic resonance imaging has become a standard exam for pre and post-treatment of aortic coarctation. It takes place immediately after Doppler echocardiography and must include numerous sequences to obtain a complete evaluation. Based on our experience and in order to decrease examination time, the best MR protocol for evaluation of aortic coarctation is the following: Fast or Turbo spin-echo imaging remains the first step to evaluate morphology. Axial images are usually insufficient to demonstrate the abnormality but remain essential to demonstrate associated malformations, particularly intracardiac anomalies. Oblique sagittal images centered on aortic arch are mandatory but usually not sufficient to demonstrate the degree of narrowing; they must be completed by coronal or oblique coronal images, which are frequently more efficient for the evaluation of the degree of narrowing in the isthmus region. To decrease examination time, oblique sagittal and coronal cine images may be replaced by magnitude reconstruction of VEC cine sequence in the same planes. Cine-MIP technique can be abandoned and replaced by MRA. Complete haemodynamic evaluation includes oblique sagittal and oblique coronal VEC cines (in-plane velocity measurement) encompassing the length of the jet, with velocity encoded vertically. Planes perpendicular to the direction of the flow void (through-plane velocity measurement) on axial transverse images distal to the coarctation may be performed in cases where the measurement on the two previous planes is insufficient. At the end of the exam, 3D CE MRA must be performed with two acquisitions and reconstructions with MIP algorithm but preferentially with volume rendering and thick-slab MPR.

Severity of aortic coarctation can be judged on several parameters discussed above. Internal measurement of the narrowing by MRI is as efficient as those performed with echocardiography and angiography and is one of the parameters permitting to evaluate the severity of the malformation but does not correspond to the external aspect of the narrowing visualized during surgical repair. Conversely, measurements of aortic arch with MRI, particularly in order to demonstrate associated tubular hypoplasia are comparable with anatomic measurements.

References

1. Sechtem U. Imaging of aortic coarctation; difficult choices. Eur Heart J 1995; 16: 1315–1316.
2. Engvall J, Sjoqvist L, Nylander E, Thuomas KA, Wranne B. Biplane transoesophageal echocardiography, transthoracic Doppler, and magnetic resonance imaging in the assessment of coarctation of the aorta. Eur Heart J 1995; 16: 1399–1409.
3. Amparo EG, Higgins CB, Schafton EG. Demonstration of coarctation of the aorta by magnetic resonance imaging. AJR 1984; 143: 1192–1194.
4. Didier D, Higgins CB, Fisher MR, Osaki L, Silvermann NH, Cheitlin MD. Gated magnetic resonance imaging in congenital heart disease: experience in initial 72 patients. Radiology 1986; 158: 227–235.
5. Von Schultess GK, Higashino S, Higgins S, Didier D, Fisher M, Higgins CB. Coarctation of the aorta: MR Imaging. Radiology 1986; 158: 469–474.
6. Mohiaddin RH, Kilner PJ, Rees S, Longmore DB. Magnetic resonance volume flow and jet velocity mapping in aortic coarctation. J Am Coll Cardiol 1993; 22: 1515–1521.
7. Powell AJ, Geva T. Blood flow measurement by magnetic resonance imaging in congenital heart disease. Pediatr Cardiol 2000; 21: 47–58.
8. Bogren HG, Buonocore MH. Blood flow measurements in the aorta and major arteries with MR velocity mapping. JMRI 1994; 4: 119–130.
9. Prince MR, Narasimham DL, Jacoby WT, et al. Three-dimensional gadolinium-enhanced MR angiography of the thoracic aorta. AJR 1996; 166: 1387–1397.
10. Krinsky GA, Rofsky NM, Flyer M, et al. Thoracic aorta: comparison of Gadolinium-enhanced three-dimensional MR angiography and conventional MR imaging. Radiology 1997; 202: 183–193.
11. Smith Maia MM, Cortes TM, Parga JR, et al. Evolutional aspects of children and adolescents with surgically corrected aortic coarctation: clinical, echocardiographic, and magnetic resonance image analysis of 113 patients. J Thorac Cardiovasc Surg 2004; 127: 712–20.
12. Muhler EG, Neuerburg JM, Ruben A, et al. Evaluation of aortic coarctation after surgical repair: role of magnetic resonance imaging and Doppler ultrasound. Br Heart J 1993; 70: 285–90.
13. Bogaert J, Kuzo R, Dymarkowski S, et al. Follow-up of patients with previous treatment for coarctation of the thoracic aorta: comparison between contrast-enhanced MR angiography and fast spin-echo MR imaging. Eur Radiol 2000; 10: 1847–54.
14. Didier D, Ratib O, Friedli B, et al. Cine gradient-echo MR imaging in the evaluation of cardiovascular diseases. Radio Graphics 1993; 13: 561–573.
15. Didier D, Ratib O, Beghetti M, Oberhaensli I, Friedli B. Morphologic and functional evaluation of congenital heart disease by magnetic resonance imaging. J Magn Reson Imaging 1999; 10: 639–55.
16. Lim DS, Ralston MA. Echocardiographic indices of Doppler flow patterns compared with MRI or angiographic measurements to detect significant coarctation of the aorta. Echocardiography 2002; 19: 55–60.
17. Carvalho JS, Redington AN, Shinebourne EA, Rigby ML, Gibson D. Continuous wave Doppler echocardiography and coarctation of the aorta: gradients and flow patterns in the assessment of severity. Br Heart J 1990; 64: 133–7.
18. Glancy DL, Morrow AG, Simon AL, Roberts WC. Juxtaductal aortic coarctation. Analysis of 84 patients studied hemodynamically, angiographically, and morphologically after age 1 year. Am J Cardiol 1983; 51: 537–51.
19. Pinzon JL, Burrows PE, Benson LN, et al. Repair of coarctation of the aorta in children: postoperative morphology. Radiology 1991; 180: 199–203.
20. Bogaert J, Gewillig M, Rademakers F, et al. Transverse arch hypoplasia predisposes to aneurysm formation at the repair site after patch angioplasty for coarctation of the aorta. J Am Coll Cardiol 1995; 26: 521–7.
21. Gutberlet M, Hosten N, Vogel M, et al. Quantification of morphologic and hemodynamic severity of coarctation of the aorta by magnetic resonance imaging. Cardiol Young 2001; 11: 512–20.
22. Soler R, Rodriguez E, Requejo I, Fernandez R, Raposo I. Magnetic resonance imaging of congenital abnormalities of the thoracic aorta. Eur Radiol 1998; 8: 540–6.
23. Weinberg PM, Fogel MA. Cardiac MR imaging in congenital heart disease. Cardiol Clin 1998; 16: 315–48.
24. Greenberg SB, Marks LA, Eshaghpour EE. Evaluation of magnetic resonance imaging in coarctation of the aorta: the importance of multiple imaging planes. Pediatr Cardiol 1997; 18: 345–9.
25. Simpson IA, Chung KJ, Glass RF, Sahn DJ, Sherman FS, Hesselink J. Cine magnetic resonance imaging for evaluation of anatomy and flow relations in infants and children with coarctation of the aorta. Circulation 1988; 78: 142–8.
26. Castillo E, Lima JA, Bluemke DA. Regional myocardial function: advances in MR imaging and analysis. Radiographics 2003; 23: S127–40.
27. Di Cesare E, Giordano AV, Cerone G, Splendiani A, Michelini O, Masciocchi C. 3-dimensional magnetic resonance angiography in apnea with the rapid infusion of a paramagnetic contrast medium in studying the thoracic aorta. Radiol Med 1999; 98: 361–7.
28. Ho VB, Prince MR. Thoracic MR aortography: imaging techniques and strategies. Radiographics 1998; 18: 287–309.
29. Godart F, Labrot G, Devos P, McFadden E, Rey C, Beregi JP. Coarctation of the aorta: comparison of aortic dimensions between conventional MR imaging, 3D MR angiography, and conventional angiography. Eur Radiol 2002; 12: 2034–9.
30. Okuda S, Kikinis R, Geva T, Chung T, Dumanil H, Powell AJ. 3D-shaded surface rendering of gadolinium-enhanced MR angiography in congenital heart disease. Pediatr Radiol 2000; 30: 540–5.
31. Stern HC, Locher D, Wallnofer K, et al. Noninvasive assessment of coarctation of the aorta: comparative

measurements by two-dimensional echocardiography, magnetic resonance, and angiography. Pediatr Cardiol 1991; 12: 1–5.
32. Mendelsohn AM, Banerjee A, Donnelly LF, Schwartz DC. Is echocardiography or magnetic resonance imaging superior for precoarctation angioplasty evaluation?. Cathet Cardiovasc Diagn 1997; 42: 26–30.
33. Rebergen SA, van der Wall EE, Doornbos J, et al. Magnetic resonance measurements of velocity and flow: Technique, validation and cardiovascular applications. Am Heart J 1993; 126: 1439–1456.
34. Bogren HG, Buonocore MH. Blood flow measurements in the aorta and major arteries with MR velocity mapping. J Magn Reson Imaging 1994; 4: 119–30.
35. Szolar DH, Sakuma H, Higgins CB. Cardiovascular applications of magnetic resonance flow and velocity measurements. J Magn Reson Imaging 1996; 6: 78–89.
36. Firmin D, Underwood R Magnetic resonance flow imaging. In: Underwood R, Firmin D (eds), Magnetic Resonance of the Cardiovascular SystemOxford. Blackwell Scientific Publications, Oxford 1991.
37. Higgins CB, Sakuma H. Heart disease: Functional evaluation with MR imaging. Radiology 1996; 199: 307–315.
38. Mohiaddin RH, Pennell DJ. MR blood flow measurement. Clinical application in the heart and circulation. Cardiol Clin 1998; 16: 161–187.
39. Henk CB, Grampp S, Koller J, et al. Elimination of errors caused by first-order aliasing in velocity encoded cine-MR measurements of postoperative jets after aortic coarctation: in vitro and in vivo validation. Eur Radiol 2002; 12: 1523–31.
40. Marx GR, Allen HD. Accuracy and pitfalls of Doppler evaluation of the pressure gradient in aortic coarctation. J Am Coll Cardiol 1986; 7: 1379–85.
41. Levine RA, Jimoh A, Cape EG, McMillan S, Yoganathan AP, Weyman AE. Pressure recovery distal to a stenosis: potential cause of gradient ''overestimation'' by Doppler echocardiography. J Am Coll Cardiol 1989; 13: 706–15.
42. Holmqvist C, Stahlberg F, Hanseus K, et al. Collateral flow in coarctation of the aorta with magnetic resonance velocity mapping: correlation to morphological imaging of collateral vessels. J Magn Reson Imaging 2002; 15: 39–46.
43. Steffens JC, Bourne MW, Sakuma H, O'Sullivan M, Higgins CB. Quantification of collateral blood flow in coarctation of the aorta by velocity encoded cine magnetic resonance imaging. Circulation 1994; 90: 937–43.
44. Dodge-Khatami A, Backer CL, Mavroudis C. Risk factors for recoarctation and results of reoperation: a 40-year review. J Card Surg 2000; 15: 369–77.
45. De Mey S, Segers P, Coomans I, Verhaaren H, Verdonck P. Limitations of Doppler echocardiography for the postoperative evaluation of aortic coarctation. J Biomech 2001; 34: 951–60.
46. Therrien J, Thorne SA, Wright A, Kilner PJ, Somerville J. Repaired coarctation: a ''cost-effective'' approach to identify complications in adults. J Am Coll Cardiol 2000; 35: 997–1002.
47. Oshinski JN, Parks WJ, Markou CP, et al. Improved measurement of pressure gradients in aortic coarctation by magnetic resonance imaging. J Am Coll Cardiol 1996; 28: 1818–26.

Address for correspondence: D. Didier, Department of Radiology, Hôpital Cantonal Universitaire de Genève, 24 rue Micheli du Crest, 1211, Geneva 14, Switzerland
Tel.: +41-22-372-70-32; Fax: +41-22-372-70-72
E-mail: dominique.didier@sim.hcuge.ch